Nanoscale Res Lett (2009) 4:420–430
DOI 10.1007/s11671-009-9262-5

NANO EXPRESS

Influence of Nanogels on Mechanical, Dynamic Mechanical, and Thermal Properties of Elastomers

Suman Mitra · Santanu Chattopadhyay · Anil K. Bhowmick

Received: 6 October 2008 / Accepted: 27 January 2009 / Published online: 13 February 2009

Abstract Use of sulfur crosslinked nanogels to improve various properties of virgin elastomers was investigated for the first time. Natural rubber (NR) and styrene butadiene rubber (SBR) nanogels were prepared by prevulcanization of the respective rubber lattices. These nanogels were characterized by dynamic light scattering, atomic force microscopy (AFM), solvent swelling, mechanical, and dynamic mechanical property measurements. Intermixing of gel and matrix at various ratios was carried out. Addition of NR gels greatly improved the green strength of SBR, whereas presence of SBR nanogels induced greater thermal stability in NR. For example, addition of 16 phr of NR gel increased the maximum tensile stress value of neat SBR by more than 48%. Noticeable increase in glass transition temperature of the gel filled systems was also observed. Morphology of these gel filled elastomers was studied by a combination of energy dispersive X-ray mapping, transmission electron microscopy, and AFM techniques. Particulate filler composite reinforcement models were used to understand the reinforcement mechanism of these nanogels.

Keywords Nanogels · Elastomers · Gels · Mechanical properties · Thermal properties

Electronic supplementary material The online version of this article (doi:10.1007/s11671-009-9262-5) contains supplementary material, which is available to authorized users.

S. Mitra · S. Chattopadhyay · A. K. Bhowmick (✉)
Rubber Technology Centre, Indian Institute of Technology, Kharagpur 721302, India
e-mail: anilkb@rtc.iitkgp.ernet.in

Introduction

Virgin polymers, especially elastomers have inherently low stiffness and strength. In order to overcome these obvious limitations and to expand their applications in different fields, particulate fillers, such as carbon black, silica, glass, calcium carbonates, carbon nanotubes, nano clays etc. are often added to polymer. Particulate fillers modify physical and mechanical properties of polymers in many ways. Use of carbon black for improving reinforcement properties of an elastomer has been studied extensively in numerous investigations [1, 2]. Amongst the nonblack fillers, mostly silica provides the best reinforcing properties [3]. In the last decade, it has been shown that dramatic improvements in mechanical and other properties can be achieved by incorporation of a few weight percentages (wt%) of inorganic exfoliated clay minerals consisting of mostly layered silicates in polymer matrices [4–10]. These are better known as polymer nanocomposites. Similar enhancements in various properties have also been reported with other types of nanofillers e.g. multiwalled carbon nanotubes and layered double hydroxides [11, 12].

Although not strictly categorized as filler, use of gels to improve various physical properties of elastomers, with an added advantage of superior processability, can be found in the prevailing literature [13–15]. Kawahara et al. [16] have reported the effect of gel on green strength of natural rubber. In most of the above work, the authors have used physically crosslinked or entangled network gels. However, our recent preliminary work with chemically crosslinked nanogels and quasi-nanogels has revealed that addition of these gels leads to a considerable improvement in processability, mechanical, and dynamic mechanical properties of virgin natural rubber (NR) and styrene butadiene rubber (SBR) [17–19]. Optimization of these

as-prepared crosslinked gels has been carried out by measuring various physical properties including crosslink density and the optimum level of gel loading has been determined from the rheological properties of the gel filled systems [17, 19]. However, the extent of property enhancement upon the addition of chemically crosslinked gels varies with the nature of matrix and gels. In the present work, our aim was to improve the deficiency in virgin NR property by using SBR nanogels and vice versa. For example, we have attempted to improve the thermal stability of NR using SBR gels which have inherently better thermal stability, without sacrificing any other properties. Similarly, green strength of SBR can be improved greatly by using the relatively high strength NR gels. For this purpose, NR and SBR latex nanogels having gradient of crosslink density and different particle sizes were prepared by sulfur prevulcanization technique and thoroughly characterized. These latex gels were then intermixed with neat NR and SBR lattices at different loadings. Finally, influence of these chemically crosslinked gels on mechanical, dynamic mechanical, and thermal behavior of virgin elastomers was studied in detail along with an extensive morphological study, for the first time.

Experimental

Materials

High ammonia centrifuged natural rubber (NR) latex having 60% dry rubber content (DRC) was provided as free sample by the Rubber Board, Kottayam, India. Sulfur, zinc oxide (ZnO), and zinc diethyl dithiocarbamate (ZDC), all in 50% aqueous dispersion, were also obtained from the same source and used as received. Styrene butadiene rubber (SBR) latex having 30% total solid content (T.S·C) and 30% bound styrene content, with a pH of 10.5 was generously received as gift sample from the Apar Industries, Ankeleswar, India. Toluene (LR-grade), potassium hydroxide (KOH), and potassium laurate ($KC_{12}H_{23}O_2$) were procured from s.d. Fine Chemicals, Mumbai, India. Doubly distilled water was obtained from indigenous source.

Preparation of Sulfur Prevulcanized Latex Gel and Gel Filled Rubber

Chemically crosslinked NR latex and SBR latex gels were prepared by employing sulfur prevulcanization technique. The virgin lattices were compounded with S, ZDC, and ZnO dispersions and subsequently prevulcanized. The formulations of different mixes for sulfur prevulcanization are given in Table 1. Sulfur to accelerator ratio was varied from 0.5 to 3 in the crosslinking recipes. Vulcanization reaction of the compounded latex was carried out at 80 °C for 2 h; the detailed procedure was described in our earlier communications [17, 19]. Films of crosslinked gel were obtained from prevulcanized latex by casting on a level glass plate and subsequent drying at ambient temperature (25 ± 2 °C) to constant weight. Finally, the films were vacuum dried at 50 °C for 12 h. These films were used for characterization of gelled rubber.

Intermixing of gel filled raw rubber samples was carried out by adding a given amount of a particular type of NR latex gel to virgin SBR latex and vice versa, followed by gentle stirring (200–300 rpm) for 1 h at 25 ± 2 °C. Then, these were cast and dried following the above-mentioned procedure. These gel filled raw rubber films were used for further testing.

Sample Designations

Control natural rubber latex and styrene butadiene rubber latex were designated as NR and SBR, respectively. Individual NR and SBR gels were expressed as NS_a and SBS_a, respectively, where '*a*' represents the ratio of sulfur to accelerator used in the prevulcanization recipe. NR gel mixed SBR systems were denoted as $SBNS_{a/b}$, where '*a*' has the same notation as stated above and '*b*' is the amount (phr) of prevulcanized NR gel added into the SBR latex. Similarly, SBR gel filled NR latex systems were noted as $NRSBS_{a/c}$, where '*a*' has the same meaning as stated above

Table 1 Formulations for sulfur prevulcanization

Ingredients (dry wt basis)	$NS_{0.5}$	NS_1	NS_2	NS_3	$SBS_{0.5}$	SBS_1	SBS_2	SBS_3
NR latex (60%)	100.00	100.00	100.00	100.00	0.0	0.0	0.0	0.0
SBR latex (30%)	0.0	0.0	0.0	0.0	100.00	100.00	100.00	100.00
10% KOH	0.25	0.25	0.25	0.25	0.0	0.0	0.0	0.0
10% potassium laurate	0.25	0.25	0.25	0.25	0.0	0.0	0.0	0.0
50% sulfur dispersion	0.60	1.20	1.20	1.80	0.60	1.20	2.40	3.60
50% ZDC dispersion	1.20	1.20	0.60	0.60	1.20	1.20	1.20	1.20
50% ZnO dispersion	0.20	0.20	0.20	0.20	0.20	0.20	0.20	0.20

and '*c*' is the amount (phr) of prevulcanized SBR gel added into the NR latex.

Characterization of Gelled Latex Samples and Measurements of Various Properties of Gel Filled Rubbers

Gel fraction of the prevulcanized latex films was measured by immersing the samples in toluene at room temperature (25 ± 2 °C) for 48 h (equilibrium swelling time that was determined from the experiments), and calculated from the weight of the samples before and after swelling as follows:

$$\text{Gel fraction} = W_2/W_1 \tag{1}$$

where W_1 is the initial weight of the polymer and W_2, the weight of the insoluble portion of the polymer. The results reported here are the averages of three samples.

Crosslink density, which is defined as the number of network chains per unit volume, was determined from initial weight, equilibrium swollen weight, and final deswollen weight of the sample swollen in toluene. The number of crosslink points, v per cm^3, was calculated using the well-known Flory–Rehner equation [20]:

$$v = \frac{-1}{V}\left[\frac{\ln(1-\upsilon_r)+\upsilon_r+\chi_1\upsilon_r^2}{\upsilon_r^{\frac{1}{3}}-\frac{\upsilon_r}{2}}\right] \tag{2}$$

where χ_1 is the polymer–solvent interaction parameter, V, the molar volume of the solvent, and υ_r, the volume fraction of the rubber in the swollen gel. υ_r was calculated using the following equation [21]:

$$\upsilon_r = \frac{(D_S - F_f A_w)\rho_r^{-1}}{(D_S - F_f A_w)\rho_r^{-1} + A_s\rho_s^{-1}} \tag{3}$$

where D_s, F_f, A_w, A_s, ρ_r, and ρ_s are deswollen weight of the sample, fraction insoluble, sample weight, weight of the absorbed solvent corrected for swelling increment, density of rubber, and density of solvent, respectively.

Dynamic light scattering (DLS) technique was used for the measurement of particle size of gels and their distribution. Before testing, the latex samples were diluted to 0.1 g/L concentration level using doubly distilled water. The DLS studies were carried out in Zetasizer Nano-ZS (Malvern Instrument Ltd, Worcestershire, UK) with a He–Ne laser of 632.8 nm wavelength. The data were analyzed by in-built machine software. The mean hydrodynamic particle diameter (Z_{avg}) was directly obtained from the machine software (as per ISO 13321).

The energy dispersive X-ray sulfur (S) mapping of the gel filled raw rubber systems was recorded in Oxford ISIS 300 EDX system (Oxford Instruments, Oxfordshire, UK) attached to the JSM 5800 (JEOL Ltd., Tokyo, Japan) scanning electron microscope operating at an accelerating voltage of 20 kV. The scan size in all the specimens was 10 square microns with a 200× magnification. The white points in the figures denote sulfur signals.

The morphology of the gel particles, as well as the gel filled matrices was analyzed with the help of atomic force microscopy (AFM). AFM studies were carried out in air at ambient conditions (25 °C, 60% RH) using multimode AFM, from Veeco Digital Instruments, Santa Barbara, CA, USA. Topographic height and phase images were recorded in the tapping mode AFM with the set point ratio of 0.9, using silicon tip having spring constant of 40 N/m. The cantilever was oscillated at it resonance frequency of ~280 kHz. Scanning was done at least 3 different positions of each sample and the representative images were taken. The latex gel samples were diluted several times before testing with doubly distilled water. A drop of this diluted sample was placed on a freshly cleaved mica surface which was allowed to dry before taking the image. In the case of gel filled matrices, very thin cast film samples were used for morphology. Due to the difference in their elastic modulus, one of the phases appears darker (NR) and the other one brighter (SBR) in all the AFM micrographs.

The gel filled rubber samples for transmission electron microscopy (TEM) analysis were prepared by ultra-cryomicrotomy using Leica Ultracut UCT, at around 30 °C below the glass transition temperature of the compounds. Freshly cut glass knives with cutting edge of 45° were used to get the cryosections of 50-nm thickness. The microscopy was performed using JEM-2100 (JEOL Ltd., Tokyo, Japan) operating at an accelerating voltage of 200 kV.

For the measurement of mechanical properties of the neat matrix, individual gels and gel filled matrices, tensile specimens were punched out from the cast sheets of 1 mm thickness, using ASTM Die-C. The tests were carried out as per the ASTM D 412-98 method in a universal testing machine, Zwick Roell Z010 (Zwick Roell, Ulm, Germany), at a crosshead speed of 500 mm per min at 25 ± 1 °C. TestXpert II software (Zwick Roell, Ulm, Germany) was used for data acquisition and analysis. The average of three tests is reported here. The experimental error was within ±1% for tensile strength and modulus, and within ±3% for elongation at break values.

Dynamic mechanical properties of gels, as well as gel filled rubbers were measured as a function of temperature using the Dynamic Mechanical Analyzer DMA Q800 (TA Instruments, Luken's Drive, New Castle, DE, USA). The measurements were taken under film-tension mode in the appropriate temperature range with a heating rate of 3 °C/min and at 1 Hz frequency. The peak value of Tan δ curves was taken as the glass transition temperature (T_g). Thermal Advantage software (TA Instruments, Newcastle, Delaware) was used for data acquisition and analysis.

Thermogravimetric analysis (TGA) of gel filled systems was done using TA Instruments (Luken's Drive, New Castle, DE, USA) TGA-Q 50. The samples (10 ± 2 mg) were heated from ambient temperature to 700 °C in the furnace of the instrument under nitrogen atmosphere at a flow rate of 60 mL/min. The experiments were done at 10 °C/min heating rate and the data of weight loss versus temperature were recorded online in the TA Instrument's Q series Explorer software. The analysis of the thermogravimetric (TG) and derivative thermogravimetric (DTG) curves was done using TA Instrument's Universal Analysis 2000 software version 3.3B. In the present study, the temperature corresponding to 5% weight loss was taken as initial degradation temperature (T_i) and the temperature corresponding to the maximum rate of degradation in the derivative thermogram was considered as peak degradation temperature (T_{max}). The experimental error limit was within ± 1 °C.

Results and Discussion

Characterization of Crosslinked Nanogels

Figure 1a–b compares the particle size distribution (PSD) of the control SBR and NR lattices and their sulfur prevulcanized gels, as determined by the DLS method, respectively. The gels and the virgin SBR latex show wide PSD with particle diameters ranging from 35 to 139 nm (Fig. 1a). In the case of NR latex gels, it reveals also a broad distribution of particle sizes for all the systems studied, with a size range of 122–360 nm, which is within the expected size range reported in the literature [22]. Apparently, both the NR and SBR gels give very similar PSD than that of their respective control latex. Z_{avg} values, the mean hydrodynamic particle diameter, of SBR and NR latex gels are listed in Table 2. The Z_{avg} for NR gels lies between 205 nm and 221 nm as against 220 nm of the control NR latex. For SBR gels, these values range from 87 to 94 nm, while Z_{avg} of SBR latex is 85 nm. PSD and Z_{avg} do not change much during the course of prevulcanization reaction. This is believed to be due to the fact that sulfur crosslinking during prevulcanization occurs inside the individual latex particles and does not alter the Z_{avg} and the PSD greatly [23]. The increase in sulfur to accelerator ratio has no apparent effect on the dimensions of the gel particles, although there is a slight increase in Z_{avg} for SBS gels without any particular trend.

Tapping mode atomic force microscopy (AFM) technique was used to visualize the individual gel particles, as illustrated in Fig. 2a–b. Here, NS_3 and SBS_3 gels have been shown as representative systems. The particle diameters in

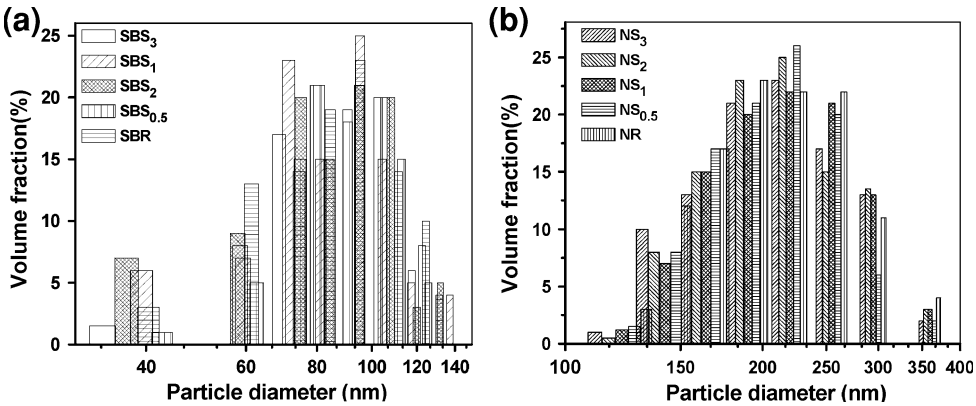

Fig. 1 Particle size distribution by DLS method for **a** SBR and SBS gels and **b** NR and NS gels

Table 2 Various properties of the gels

Gel type	*Z*-avg diameter (nm)	Gel content (%)	Crosslink density × 10^4 (gmolcm^{-3})	T.S. (MPa)	Young's modulus (MPa)	E.B. (%)	E' at 25 °C (MPa)	T_g (°C)
$NS_{0.5}$	205	88.0	0.36	12.7	1.30	1200	1.56	−53.4
NS_1	219	94.2	0.75	15.8	1.45	1170	1.65	−51.6
NS_2	214	96.3	1.00	17.0	1.74	1125	2.10	−50.5
NS_3	221	97.4	1.11	18.9	1.98	1120	2.42	−48.6
$SBS_{0.5}$	94	89.0	0.80	2.1	3.04	430	0.80	−38.0
SBS_1	92	92.5	1.50	2.8	3.42	405	1.28	−37.1
SBS_2	87	95.1	2.20	3.1	3.85	370	2.31	−35.9
SBS_3	90	97.0	2.40	3.2	3.90	360	2.63	−31.0

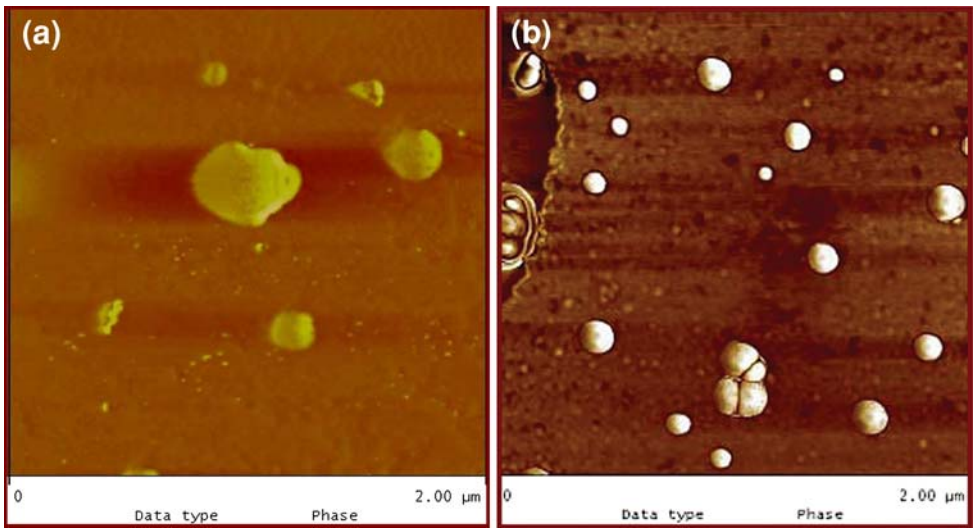

Fig. 2 AFM phase image showing morphology of **a** NS_3 and **b** SBS_3 gel particles (Scan size 2 µm × 2 µm)

the case of SBS_3 vary from 40 to 150 nm (Fig. 2b) with most of the gel particles having ~100 nm diameter, which is in line with the earlier DLS findings. These gel particles are nearly spherical in shape. In the case of NS_1 (Fig. 2a), even broader distribution in particle sizes can be seen in the AFM image.

The values of gel content and crosslink density for all the crosslinked gels are tabulated in Table 2. With the increase in sulfur to accelerator ratio, both gel content and crosslink density increase for SBS as well NS gel systems. $SBS_{0.5}$ has a gel content of 89%, which increases up to 97% in SBS_3. A similar trend is also observed for crosslink density (0.8×10^{-4}gmol/cc for $SB_{0.5}$ to 2.4×10^{-4}gmol/cc for SB_3). A comparable increase in gel content and crosslink density is observed for NR gels. The increment in gel content and crosslink density values with increasing sulfur to accelerator ratio can be attributed to the formation of sulfide linkages between the molecules, which lead to a three-dimensional network structure. However, as the sulfur to accelerator ratio increases from 2 to 3, the increase in the amount of crosslinking tends to level off, as evident from gel content and crosslink density values of SBS_2/SBS_3 and NS_2/NS_3 systems. This is because of the saturation of sites available for crosslinking. Although the gel content values are quite close for both SBS and NS types of gels at any given sulfur to accelerator ratio, SBR gels show almost double the amount of crosslinking than their NR gel counterparts. Because of the nano size of SBR latex particles compared to the NR latex, higher available surface area in nano latex particle leads to the efficient diffusion of these curing agents during prevulcanization and hence higher amount of crosslinking.

The effect of sulfur crosslinking is also very pronounced on the mechanical properties of different gels as compared to their virgin counter parts. The mechanical properties of the gelled lattices are reported in Table 2. The maximum tensile stress of the control SBR latex (SB), which is only 0.29 MPa, shows many fold increase after sulfur crosslinking. The elongation at break (EB) value of neat SBR is 700%, which decreases considerably upon crosslinking to 360% in SBS_3. The tensile strength (TS) increases steadily, while the EB value decreases consistently with the increase in amount of sulfur in the system. Increase in T.S. and reduction in EB values are related to the introduction of greater number of crosslinks initiated by the sulfide linkages. In the case of NS series of gels, TS value increases by more than 10 times from 1.86 MPa in NR to 18.9 MPa in NS_3 gel with a concomitant decrease in EB from 1400% in NR to 1120% in NS_3. The trend in Young's modulus (E_y) values is very similar to that of TS. However, SBR gels have comparatively higher values of E_y than the NR gels.

The dynamic mechanical properties of different gels as compared to that of neat rubber strongly reflect the influence of crosslinking. With the increase in sulfur to accelerator ratio, tan δ peak (considered as T_g here) shifts toward higher temperature (Table 2). It is worth mentioning here that the neat NR has a T_g of about −56 °C and that of SBR is −39 °C. Hence, considerable increase in T_g with the introduction of crosslinking in the rubber matrix can be seen along with the broadening of tan δ peak height (not shown here). In the case of NR gels, T_g shifts by more than +7 °C (from NR to NS_3), while for SBR gels, there is a +8 °C shift from SBR to SBS_3. The increase in T_g values with the progressive increase in sulfur to accelerator ratio can be ascribed to the restriction imposed on the chain movement due to the crosslinking, as there is lesser number of free chains available to execute unrestricted segmental motion. The storage modulus (E') values at 25 °C are also reported in Table 2 for the gels used in this study. As in the case of tensile modulus, E' also increases steadily with

increase in amount of crosslinking. $SBS_{0.5}$ has an E' value of 0.8 MPa, which increases by more than threefold to 2.63 MPa for SBS_3. Similar observations are also noted for NR gels; however, the level of increment in modulus values is less as compared to SBR gels.

These nanogels were subsequently used as viscoelastic fillers for the inter mixing study i.e. NS gels were added to SBR matrix and SBS gels were mixed with NR at a given concentration, to investigate their effect on the morphology, mechanical, dynamic mechanical and thermal properties of raw SBR and NR.

Morphology of the Gel Filled Rubbers

EDX or energy dispersive X-ray sulfur mapping is a useful technique to check the distribution of gel particles in the rubber matrix. Figure 3a–d shows representative EDX images of 4 and 16 phr gel loaded SBR and NR matrices. It is quite apparent that at 4 phr loading, the gels are very well distributed irrespective of the nature of the gels or the matrix. For example, both $SBNS_{1/4}$ and $NRSBS_{1/4}$ (Fig. 3a and c) show good distribution of NS and SBS gels in the neat SBR and NR, respectively. However, the scenario changes completely in the case of 16 phr gel filled samples. Both the $SBNS_{1/16}$ and the $NRSBS_{1/16}$ show (Fig. 3b and d) considerable agglomeration of gel particles. EDX study also clearly demonstrates that aggregation in nanosized SBS_1 gel filled system is more than that in NS_1 gel filled system.

The surface morphology of the gel filled samples has been investigated with atomic force microscopy in tapping

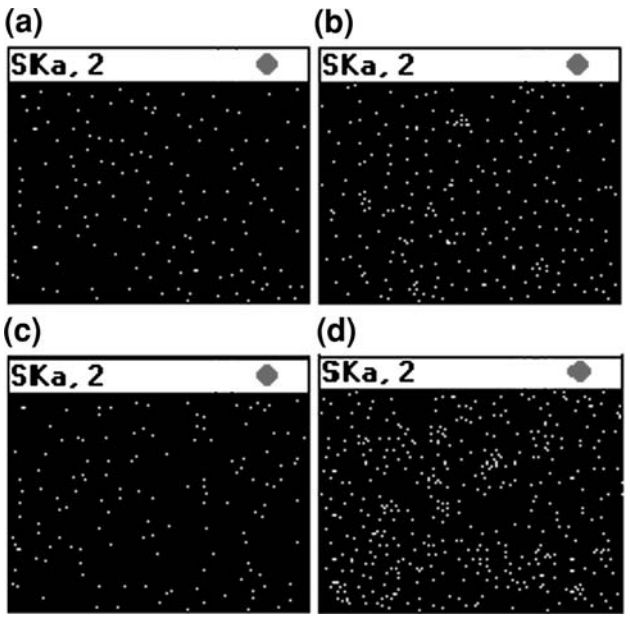

Fig. 3 EDX-sulfur mapping showing gels distribution in matrix for **a** $SBNS_{1/4}$, **b** $SBNS_{1/16}$, **c** $NRSBS_{1/4}$, and **d** $NRSBS_{1/16}$

mode by magnifying a small region of the surface. These are shown in Fig. 4a–d. In this mode, more rigid component appears as the brighter spots on the phase image and the darker regions correspond to a less rigid component [24]. Although taken at a much smaller scan size of 5 μ, these AFM images are perfectly in line with the earlier EDX observation. In Fig. 4a, NS_1 gels at 4 phr loading in SBR matrix can be seen as dark colored circular and semi-circular dispersed domains. Individual gel particles are fairly uniformly distributed (circular) with occasional one or two gel agglomerate (semi-circular). The domain sizes of most of the single gel particles range from 130 to 360 nm, which corroborates the earlier DLS and AFM findings. For $NRSBS_{1/4}$, as shown in Fig. 4b, again homogeneous distribution of nanogels (brighter circular spots) in NR matrix is observed. Most of the gel particles have sizes ranging from 70–130 nm. This again shows good correlation with the PSD data obtained from the DLS measurements. However, it can be seen that, nano SBS_1 gels at even 4 phr loading in NR show some sign of agglomeration, with circular domains of aggregated particles of 250–350 nm. At 16 phr loading, both $SBNS_{1/16}$ and $NRSBS_{1/16}$ display regions having agglomerated gel particles with domain size much larger than the individual particles (Fig. 4c–d). In the case of $SBNS_{1/16}$ system (Fig. 4c), NS_1 gel agglomerates having dispersed domains ranging from 500 to 770 nm in length can be detected easily. These are comprised of at the most 2–3 individual gel particles. It may be noted here that the tendency of NR gels to form agglomerates is much less compared to the nano sized SBR gels as shown in Fig. 4d for $NRSBS_{1/16}$ system. This has been shown earlier also with the help of EDX study. In 16 phr nano SBS gel loaded NR matrix, almost all the nanogels are in agglomerated state having dispersed gel domains of 300 to 1500 nm in length. This implies that unlike NR gels, several nano sized gel particles take part in forming very large cluster of gel agglomerates. This type of agglomerating behavior of nanogel particles at comparatively higher loading is very similar to that of the nanofillers reported in literature [25]. Section analysis of representative 4 phr gel loaded samples corroborates the AFM findings about the gel domain sizes and also generates some interesting features (see Figure S1 of Supplementary Information). It shows that NR gels are embedded in the SBR matrix (less rough surface), whereas SBR nanogels appear mostly on the surface of NR matrix (more rough surface), which could be due to the differences in the gels moduli. It may be pointed out here that the AFM morphology of nanogel filled elastomers is possibly being reported for the first time.

Transmission electron microscopy (TEM) was performed to elucidate the bulk morphology of the representative gel filled samples. These are presented in Fig. 5a–d.

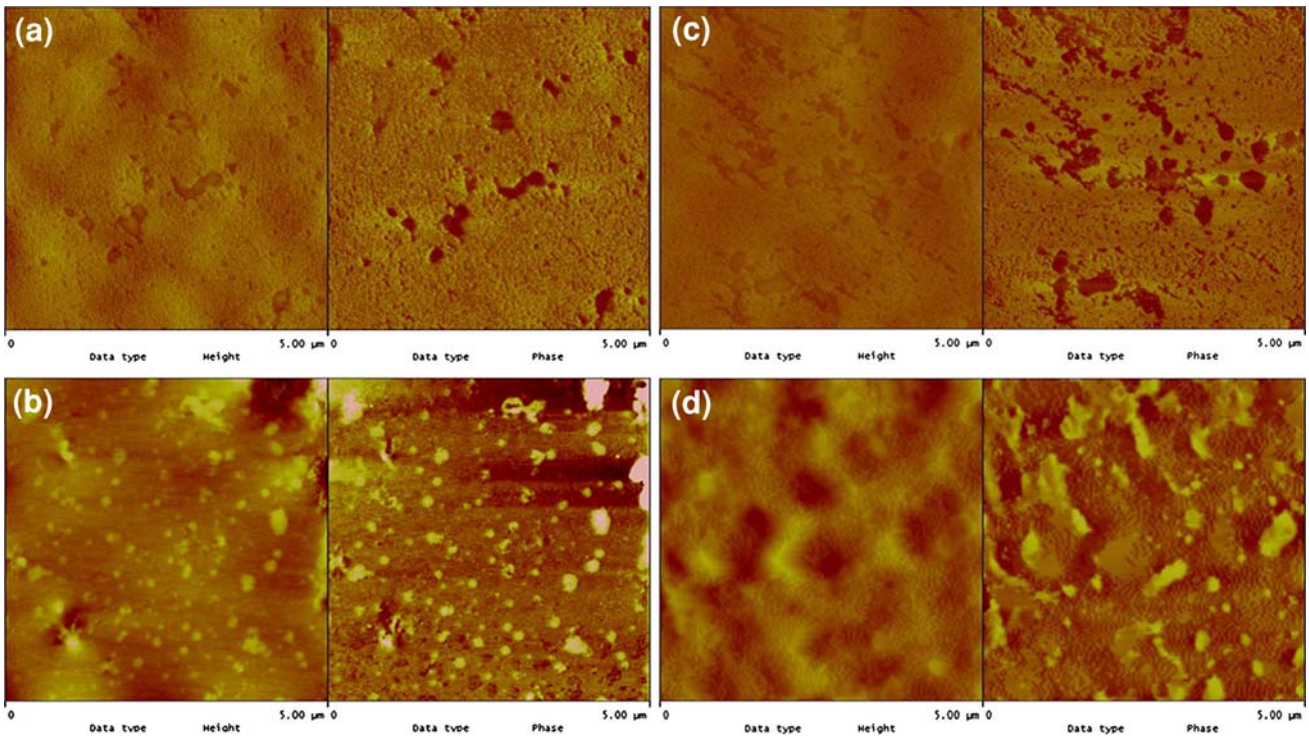

Fig. 4 Nanoscale morphology of gel filled samples by AFM (height image on the left and phase image on the right) for **a** $SBNS_{1/4}$, **b** $NRSBS_{1/4}$, **c** $SBNS_{1/16}$, and **d** $NRSBS_{1/16}$

NR gels with 200–300 nm domain size and SBR nanogels with less than 200 nm can be seen clearly in the TEM images of $SBNS_{1/4}$ and $NRSBS_{1/4}$ samples, respectively (Fig. 5a–b). However, considerable gel particle agglomeration can be seen in 16 phr SBR nanogel filled NR sample (Fig. 5d). NR gels show comparatively lesser tendency to agglomerate at higher loading (Fig. 5c). The bulk morphology as investigated from the TEM study is completely in line with the surface morphology by AFM and compliments each other well.

Effect of Gels on the Tensile Properties

The tensile properties of NS_1 gel filled SBR systems and SBS_1 gel filled NR systems are listed in Table 3. Compared to neat rubbers, all the gel filled systems exhibit improvement in tensile strength (TS) or in maximum tensile stress, F_{max} (as in the case of SBR systems due to their plastic deformation before rupture), Young's modulus (E_y), and modulus at 300% elongation with concomitant decrease in elongation at break (EB) values. It can be seen that with the increase in gel loading, irrespective of the NR or SBR gels, TS and moduli increase, whereas EB decreases consistently. For example, in $NRSBS_{1/4}$, there is an increase of about 11% in TS from neat NR, whereas it is 15% for $NRSBS_{1/16}$. Similarly, $SBNS_{1/2}$ shows an increase of more than 17% in modulus at 300% elongation compared to SBR and the same for $SBNS_{1/16}$ is more than 48%. It can be pointed out here that the NS_1 gels show much greater reinforcing capability in SBR than its SBR counterpart i.e. SBS_1 gels in NR. This may be because of the higher TS of the NS_1 (15.8 MPa) gels than the SBS_1 (2.8 MPa) that accounts for the better reinforcement. However, it is worth mentioning here that unlike in conventional fillers and nanoclays, agglomeration of gels found in 16 phr gel filled samples do not impair the TS or moduli value to that extent. This seems to be the major difference between these viscoelastic fillers and other particulate nanofillers [26, 27]. This is probably due to the fact that, while the nanofillers in the state of aggregation can act as stress concentration points in the rubber matrix, these viscoelastic gels act as a stress-dampening or dissipating medium. Due to the prevailing gradient of modulus or stiffness at the interface of particulate aggregate–polymer matrix compared to gel aggregate–polymer matrix, stress intensity will be higher in the former case. Thus, presence of gels in rubber matrix will lead to the increase in tensile property depending on the nature of chemically crosslinked gels used.

Figure 6 shows the effect of crosslink density of the SBR nanogels on their reinforcement ability in NR matrix. In this case, at a representative loading of 4 phr, tensile strength of gel filled NR systems increase steadily with the increase in crosslinking density. This change in TS and

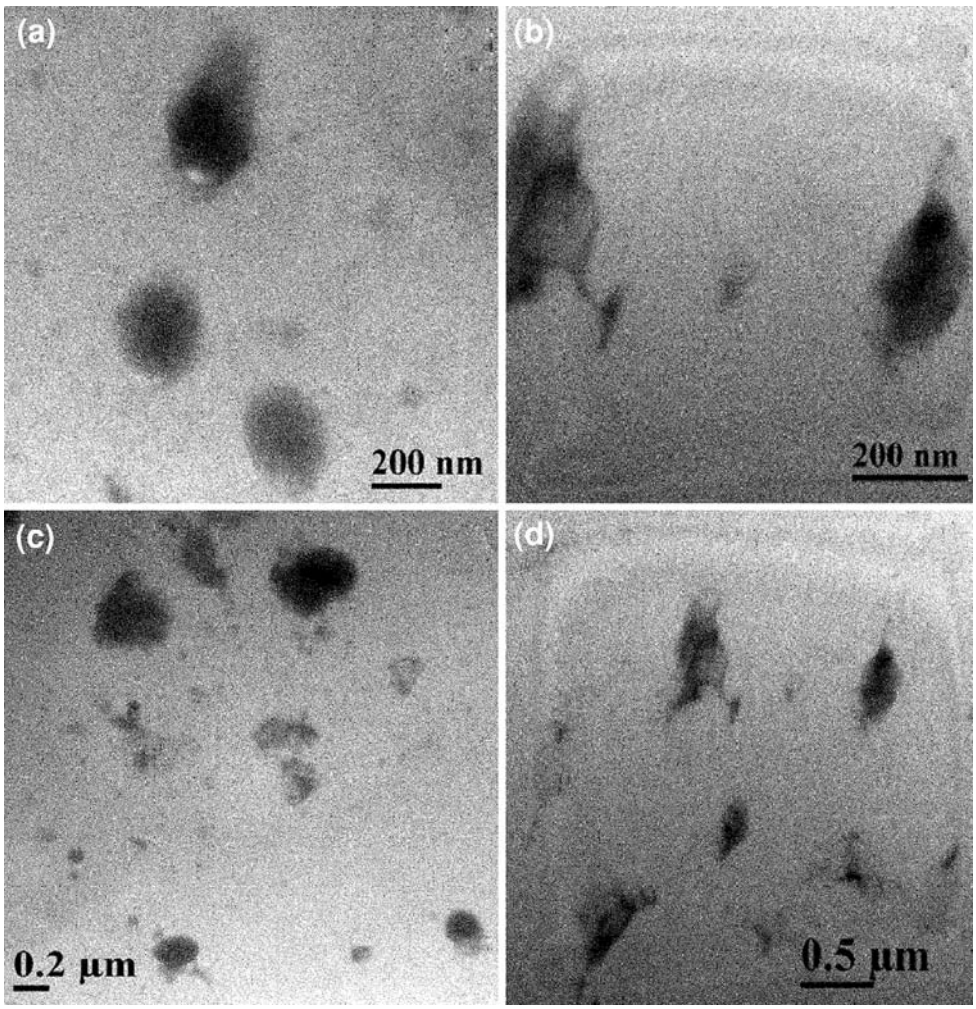

Fig. 5 Bright field TEM images of gel filled samples for **a** $SBNS_{1/4}$, **b** $NRSBS_{1/4}$, **c** $SBNS_{1/16}$, and **d** $NRSBS_{1/16}$

Table 3 Tensile properties of gel filled samples

System	T.S. (MPa)	F_{max} (MPa)	Young's modulus (MPa)	Modulus at 300% elongation (MPa)	Elongation at break (%)
NR	1.86	–	0.70	0.31	1400
$NRSBS_{1/2}$	1.97	–	0.81	0.37	1310
$NRSBS_{1/4}$	2.06	–	0.90	0.38	1300
$NRSBS_{1/8}$	2.10	–	0.96	0.41	1240
$NRSBS_{1/16}$	2.14	–	1.05	0.43	1110
SBR	–	0.29	1.36	0.29	700
$SBNS_{1/2}$	–	0.35	1.38	0.34	540
$SBNS_{1/4}$	–	0.38	1.43	0.37	430
$SBNS_{1/8}$	–	0.41	1.46	0.40	370
$SBNS_{1/16}$	–	0.43	1.53	0.43	360

modulus at 300% elongation is accompanied by substantial decrease in elongation at break. The tensile stress-elongation traces of NR and SBR systems exhibit completely different nature, as expected. In the case of SBR gel filled NR systems, very high elongation at break with a tendency to undergo strain-induced crystallization can be found (Fig. 6). However, for NS gels filled SBR (given as Figure S2 of Supplementary Information), SBR matrix show plastic deformation after attaining the maximum stress at about 100% strain level for all the systems studied. Presence of viscoelastic fillers generates considerable reinforcement without changing the inherent nature of the tensile plots. Gels with much higher TS than the neat rubber offer greater resistance to tensile deformation,

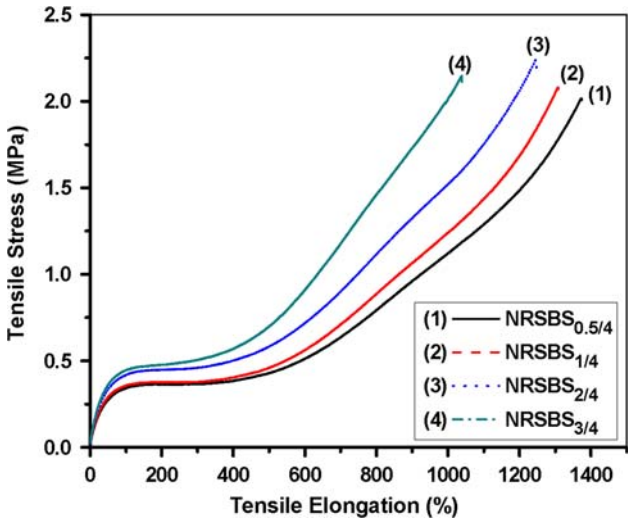

Fig. 6 Tensile stress-elongation plot of 4 phr of different SBS gels filled NR samples

thereby increasing the overall tensile strength of gel filled rubber matrix.

In order to understand the reinforcement mechanism of these nanogels in neat elastomer matrix, tensile properties of gel filled systems were analyzed in detail with the help of various particulate reinforcement models. Normally, introduction of particulate fillers in a rubber matrix leads to an increase in modulus of the composite material. This is due to the fact that modulus of inorganic particles is usually much higher than that of the polymer matrices; as a result the composite modulus is easily enhanced by adding particles to matrix. Many empirical or semi-empirical equations have been proposed to predict the modulus of particulate–polymer composites. Smallwood [28] introduced, for the first time, the following equation, using an analogy to the Einstein viscosity equation, viz.,

$$E_c = E_m(1 + 2.5\Phi) \tag{4}$$

where E_c and E_m are Young's modulus of composite and matrix, respectively and Φ is the volume fraction of the fillers. The constant 2.5 is applicable for spherically shaped particles.

Later, Guth [29] modified the above equation by taking into account the polymer–filler interaction, they proposed the following equation,

$$E_c = E_m\left(1 + 2.5\Phi + 14.1\Phi^2\right) \tag{5}$$

where the linear term is the stiffening effect of individual particles and the second power term is the contribution of particle–particle interaction. Another definitive equation for determining the modulus of a composite that contains spherical particulate inclusions in a matrix was proposed by Kerner [30] and is given below:

$$E_C/E_m = 1 + \frac{\phi}{(1-\phi)}\frac{15(1-\upsilon_m)}{(8-10\upsilon_m)} \tag{6}$$

where υ_m is the matrix Poisson ratio taken as 0.5 here. The equation is based on the assumption that the Young's modulus of the particulate inclusions (E_f) is greater than that of the matrix (i.e. $E_f \gg E_m$).

In the present case, the Young's moduli of the nanogel filled elastomers are compared with the calculated theoretical values following the Guth and Kerner reinforcement models. These are presented in Fig. 7a–b. It is apparent that the nano SBR gel filled NR systems show reasonable fitting with both the models, particularly with Guth model. However, in the case of NR gel filled SBR systems, the experimental data deviate considerably from their calculated counterpart. This anomaly can be explained by taking the Young's moduli of the gels into consideration. In all particulate reinforcement theories, it is assumed that there is a great difference in the respective Young's modulus values of particulate filler and neat matrix. However, in the case of present systems, sulfur crosslinked nanogels have been used which are partially deformable and their moduli are marginally higher than that of the virgin polymer. Because of the relatively large difference in modulus values between SB_1 nanogels (3.42 MPa) and neat NR (0.7 MPa), SB_1 gel filled NR systems show better matching with theoretical values.

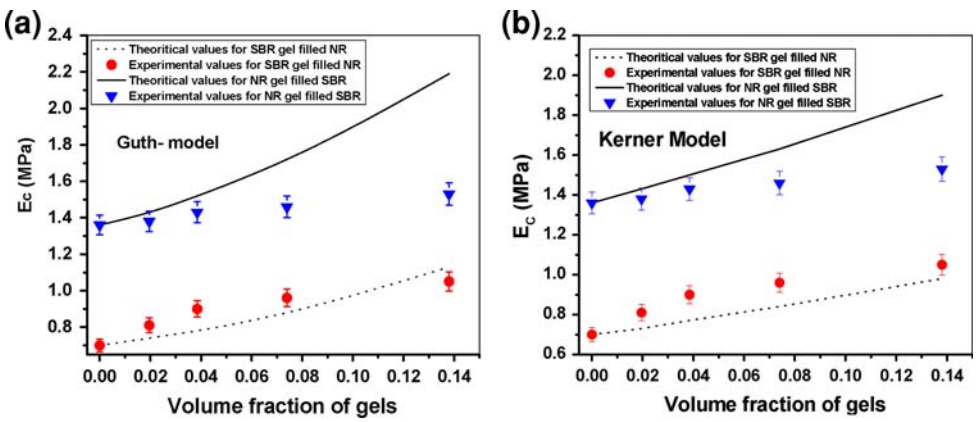

Fig. 7 Comparison between experimental and theoretical Young's modulus values for SB_1 gel filled NR and NS_1 gel filled SBR systems as determined by **a** Guth model and **b** Kerner model

Effect of Gels on the Dynamic Mechanical Properties

Figure 8 shows the temperature dependencies of storage modulus (E') for SBR nanogel filled NR systems. Over a long range of temperatures, the SBS_1 filled systems show much increased storage modulus compared to the neat NR. Again, at 25 °C, more than 1.51 times improvement in log (storage modulus) can be observed with 4 phr of NS_1 gel compared to the control SBR (shown as Figure S3 of Supplementary Information). The improvement in storage modulus is higher in the case SBS_1 filled NR systems, especially in the glassy to sub-ambient region (Fig. 8). However, in the case of NS_1 filled SBR systems, the difference in storage modulus values of gel filled systems with neat SBR is much more prominent in the rubbery plateau region, due to the lesser extent of aggregation in the case of NS_1 compared to SBS_1(Fig. S3). The storage modulus increases steadily on changing the gel loading from 2 to 16 phr in the transition region while in rubbery region, in general, it has increased marginally for SBS_1 filled NR systems. Similar trend also can be seen in NS_1 filled SBR systems. The substantial increase in storage modulus of the gel filled systems can be attributed to the presence of three-dimensional networks of crosslinked gel which provide greater resistance to dynamic deformation.

Figure 8 (inset) also illustrates the temperature dependencies of loss tangent of SBR nanogel filled NR systems. With the addition of 16 phr SBS_1 gel in NR, T_g of NR shifts towards higher temperature by 4 °C, accompanied by steady reduction in tan δ peak height. It is very interesting to mention here that upto 8 phr ($\sim$7.4 wt%) of SBS_1 gel loading in NR generates single T_g corresponding to NR. However, at 16 phr ($\sim$13.9 wt%) gel loading, two distinct peaks can been seen easily (one with a broad shoulder peak at −32.8 °C for SBS_1 gel). This could be attributed to the macro phase separation of gels with matrix at relatively higher loading. Similar trend is also observed for NS_1 filled SBR systems (see Figure S4 of Supplementary Information). For example, in $SBNS_{1/16}$, a small peak appears at −53 °C for NS_1 along with another one at −33.3 °C for SBR. With addition of NS_1 gel in SBR, T_g shifts from −39.2 °C in SBR to −32.0 °C in $SBNS_{1/8}$. The presence of crosslinks in the raw rubber matrix hinders the segmental motions of the polymer chains and therefore, T_g is progressively shifted to higher temperature with the increase in gel loading.

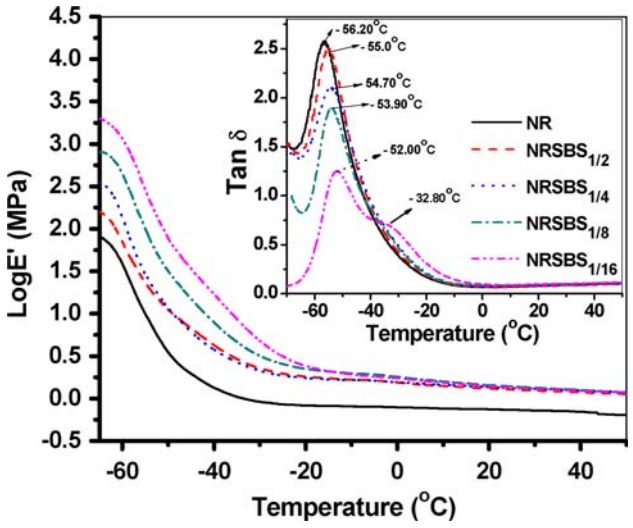

Fig. 8 Variation in Log (storage modulus) vs. temperature for SBS_1 gel filled NR systems. Variation of Tan δ (loss factor) vs. temperature for the same systems is shown as inset

Effect of Gels on the Thermal Properties

Typical TG curves for SBR nanogel filled NR is shown in Fig. 9. These TG curves correspond to predominant single-step degradation with well-defined initial and final degradation temperatures and may be a result of a random chain scission process. Normally addition of particulate fillers in neat rubber matrix is accompanied by the enhancement of thermal stability for the latter [31]. In this case also, presence of chemically crosslinked SBR nanogels improves the thermal stability of the neat NR considerably (Fig. 9). Both initial (T_i) and final decomposition (T_f, corresponding to 95% weight loss) temperature of NR increase gradually with the increase in SBR gel loading. For example, T_i (temperature corresponding to 5% weight loss) in $NRSBS_{1/16}$ increases by 9 °C from that of NR. This could be due to the inherently better thermal stability of the SBR gels compared to NR. However, in the case of NR gel filled SBR (given as Figure S5 of Supplementary Information), although there is a decrease in T_i initially with the addition

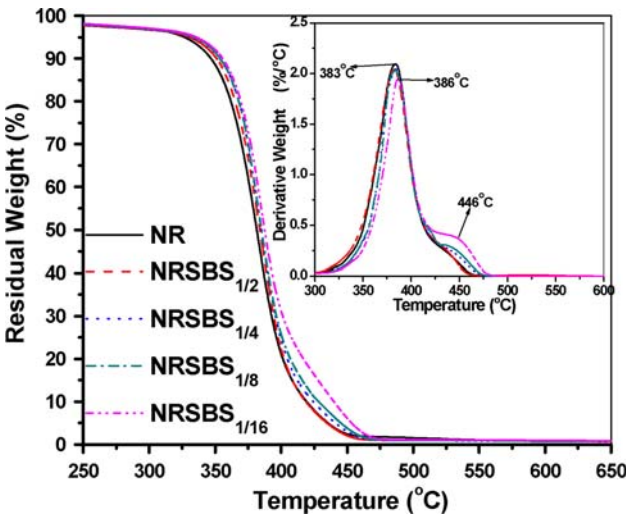

Fig. 9 TGA thermograms of SBS_1 gel filled NR systems. DTG plots of the same systems are shown as inset

of gels, the trend gets reversed at 16 phr loading. At the same time, the neat SBR and all the NR gel filled SBR systems display very close T_f values.

The DTG plots of SBS_1 nanogel filled NR also clearly demonstrate the improvement in thermal stability as shown in the inset of Fig. 9. There is 3 °C shift of T_{max} to higher temperature with addition of 16 phr SBS_1 gel in neat NR and there is a significant reduction in the rate of decomposition in the presence of the gels at major degradation step (from 2.09%/°C in NR to 1.91%/°C in $NRSBS_{1/16}$). It can be noted here that prominent 2nd peak in the DTG plots for $NRSBS_{1/8}$ and $NRSBS_{1/16}$ is due to the degradation of SBS_1 gels. Similar two stage degradation can also be seen in the NS_1 gel filled SBR systems (see Figure S6 of Supplementary Information). Addition of NS_1 gels considerably suppresses the rate of decomposition in case of neat SBR (from 1.64%/°C in neat SBR to 1.37%/°C in $SBNS_{1/16}$).

Conclusions

The use of chemically crosslinked nanogels to improve various properties of virgin elastomers has been reported for the first time. Following conclusions can be drawn from the present work. Sulfur prevulcanized nanosized latex gels have been prepared and characterized using various methods. The morphology of gel filled NR and SBR systems has been studied using X-ray dot mapping, TEM, and AFM. These show that the gels are evenly distributed at low loadings, while they tend to form agglomerates at relatively higher loadings. SBR nanogels have greater tendency for agglomeration.

Addition of chemically crosslinked nanogels also considerably improves the tensile strength and modulus of the gel filled rubbers compared to the pristine one. The tensile strength (or maximum stress) and Young's modulus increase, whereas EB decrease with the increase in nanogel loading for NR and SBR matrices. The reinforcement ability of the gels depends on their crosslinking densities. Guth and Kerner particulate reinforcement models have been used to understand the reinforcement behavior of these gels.

Presence of nanogels has shifted the T_g of neat elastomers towards higher temperature with an concomitant increase in storage modulus. Interestingly, 16 phr gels loaded samples showed two peaks in their tan δ versus temperature plots. Addition of SBR nanogels in neat NR has given rise to better thermal stability for the latter.

Acknowledgments The authors would like to thankfully acknowledge the financial assistance provided by Department of Atomic Energy (DAE), Board of Research in Nuclear Sciences (BRNS), Mumbai vide sanction no. 2005/35/4/BRNS/516 dated 08-06-2005 and also to Mr. Pradip K. Maji for the AFM measurements.

References

1. G. Kraus, *Reinforcement of Elastomers* (Interscience, New York, 1965)
2. J.B. Donnet, R.C. Bansal, M.J. Wang, *Carbon Black Science and Technology*, 2nd edn. (Marcel Dekker, New York, 1993)
3. W.H. Waddell, L.R. Evans, Rubber Chem. Technol. **69**, 377 (1996)
4. T. Lan, T.J. Pinnavaia, Chem. Mater. **6**, 2216 (1994). doi:10.1021/cm00048a006
5. E.P. Giannelis, Adv. Mater. **8**, 29 (1996). doi:10.1002/adma.19960080104
6. R.A. Vaia, E.P. Giannelis, Macromolecules **30**, 7990 (1997). doi:10.1021/ma9514333
7. J.W. Cho, D.R. Paul, Polymer (Guildf) **42**, 1083 (2001). doi:10.1016/S0032-3861(00)00380-3
8. S.S. Ray, M. Okamoto, Prog. Polym. Sci. **28**, 1539 (2003). doi:10.1016/j.progpolymsci.2003.08.002
9. S. Varghese, J. Karger-Kocsis, K.G. Gatos, Polymer (Guildf) **44**, 3977 (2003). doi:10.1016/S0032-3861(03)00358-6
10. A. Ganguly, A.K. Bhowmick, Nanoscale Res. Lett. **3**, 36 (2008). doi:10.1007/s11671-007-9111-3
11. R.P. Singh, D. Singh, R.B. Mathur, T.L. Dhami, Nanoscale Res. Lett. **3**, 444 (2008). doi:10.1007/s11671-008-9179-4
12. H. Acharya, S.K. Srivastava, A.K. Bhowmick, Nanoscale Res. Lett. **2**, 1 (2007). doi:10.1007/s11671-006-9020-x
13. W. Hofman, Rubber Chem. Technol. **7**, 85 (1964)
14. A.K. Bhowmick, J. Cho, A. MacArthur, D. McIntyre, Polymer (Guildf) **27**, 1889 (1986). doi:10.1016/0032-3861(86)90177-1
15. N. Nakajima, E.A. Collins, J. Rheol. **22**, 547 (1978)
16. S. Kawahara, Y. Isono, J.T. Sakdapipanich, Y. Tanaka, E. Aik-Hwee, Rubber Chem. Technol. **75**, 739 (2002)
17. S. Mitra, S. Chattopadhyay, A.K. Bhowmick, J. Appl, Polym. Sci. **107**, 2755 (2008)
18. S. Mitra, S. Chattopadhyay, Y.K. Bharadwaj, S. Sabharwal, A.K. Bhowmick, Radiat. Phys. Chem. **77**, 630 (2008). doi:10.1016/j.radphyschem.2007.10.006
19. S. Mitra, S. Chattopadhyay, A.K. Bhowmick, Rubber Chem. Technol. **81**(5), 842 (2008)
20. L.H. Sperling, *Introduction to Physical Polymer Science* (John Wiley & Sons Inc., New York, 1992)
21. A.K. Bhowmick, M.M. Hall, H. Benarey, *Rubber Products Manufacturing Technology* (Marcel Dekker, New York, 1994)
22. K. Sanguansap, T. Suteewong, P. Saendee, U. Buranabunya, P. Tangboriboonra, Polymer (Guildf) **46**, 1373 (2005). doi:10.1016/j.polymer.2004.11.074
23. C.C. Ho, M.C. Khew, Langmuir **15**, 6208 (1999). doi:10.1021/la981601v
24. N. Yerina, S.N. Magonov, Rubber Chem. Technol. **76**, 846 (2003)
25. M. Maiti, A.K. Bhowmick, Polymer (Guildf) **47**, 6156 (2006). doi:10.1016/j.polymer.2006.06.032
26. M. Pramanik, S.K. Srivastav, B.K. Samantaray, A.K. Bhowmick, Polym. J. Sci. Part B Polym. Phys. **40**, 2065 (2002)
27. S. Sadhu, A.K. Bhowmick, Polym. J. Sci. Part B Polym. Phys. **42**, 1573 (2004)
28. H.J. Smallwood, Rubber Chem. Technol. **21**, 667 (1948)
29. E. Guth, J. Appl. Phys. **16**, 20 (1945). doi:10.1063/1.1707495
30. E.H. Kerner, Proc. Phys. Soc. B **69**, 808 (1956). doi:10.1088/0370-1301/69/8/305
31. M. Maiti, S. Mitra, A.K. Bhowmick, Polym. Deg. Stab. **93**, 188 (2008). doi:10.1016/j.polymdegradstab.2007.10.007